



Synthesis of LaMO_3 ($M = \text{Fe}, \text{Co}, \text{Ni}$) using nitrate or nitrite molten salts

Jun Yang^{a,*}, Runsheng Li^a, Junyi Zhou^a, Xiaoci Li^a, Yuanming Zhang^a, Yulin Long^a, Yongwang Li^b

^a Department of Chemistry, Jinan University, Shipai, Guangzhou, Guangdong Province 510632, People's Republic of China

^b State Key Laboratory of Coal Conversion, Institute of Coal Chemistry, Chinese Academy of Sciences, Taiyuan 030001, People's Republic of China

ARTICLE INFO

Article history:

Received 1 July 2010

Received in revised form 2 August 2010

Accepted 21 August 2010

Available online 27 August 2010

Keywords:

Molten salt synthesis

LaMO_3

Perovskite

Basicity

ABSTRACT

Perovskite compound LaMO_3 ($M = \text{Fe}, \text{Co}, \text{Ni}$) nanocrystals were successfully synthesized in molten nitrates or nitrites from a mixture of lanthanum nitrate and an M-containing nitrate for 2 h. The effect of the various process parameters on the phase purity, crystallite size, specific surface area and morphology of the synthesized nanocrystals were systematically studied by XRD, scanning electron microscopy (SEM), simultaneous TG/DSC and BET measurements. The results showed that salt medium, annealing temperatures (mainly 450–850 °C), oxidising properties and basicity of the melt played an important role in the synthesis of LaMO_3 . The addition of Na_2O_2 facilitated the reaction between La_2O_3 and NiO or Co_3O_4 , leading to the formation of LaNiO_3 and LaCoO_3 at a much lower temperature of 450 °C. Pure hexagonal LaNiO_3 nanocrystals were obtained in molten NaNO_3 – KNO_3 eutectic with Na_2O_2 at 550–750 °C.

© 2010 Elsevier B.V. All rights reserved.

1. Introduction

Lanthanum-containing perovskite-type compounds, LaMO_3 , comprising f-transition and d-transition ions have been one of the most attractive and interesting mixed oxides due to their innovative use in advanced technologies [1]. These oxides have been used as functional materials in many fields, including solid oxide fuel cells [2,3], catalysts [4], gas separators [5], giant negative magnetoresistance [6] and various gas sensors [7,8].

The synthesis of lanthanum-containing perovskite-type oxides LaMO_3 and related compounds have been achieved by many methods involving solid-state reaction [9], mechanochemical solid reaction [10], hydrothermal synthesis [11], combustion synthesis [12,13], sol–gel method [14,15], co-precipitation method [16–19], reverse micelle method [20], polymerizable complex method [21], sonochemical method [22] and microemulsion method [23,24]. However, the conventional solid-state reaction method requires several heating and grinding steps to ensure the homogeneous mixing of the various oxides, while the reverse drop co-precipitation method requires the use of more chemicals and longer time for the formation of the LaFeO_3 [25]. To obtain desired final powders with good crystalline structures, all the wet chemical methods need a very high calcination temperature that wastes time and energy.

Chemical methods of synthesis of materials play a crucial role in the design and discovery of new materials, and provide better and less cumbersome methods for preparing known materials. It

is well known that the molten salt synthesis method is one of the simplest, most versatile, and cost-effective approaches available for obtaining a pure perovskite phase at a relatively low temperature for a shorter soaking time, in which the molten salts are used as a reaction medium. The intrinsic scalability, flexibility, and facility of this technique render it attractive for the fabrication of a range of ternary metal oxides. $\text{LaMn}_{0.8}\text{Na}_{0.2}\text{O}_3$ was produced in molten NaOH at 723 K [26]. Alkali-doped LaNiO_3 was synthesized in molten KOH at 673 K [27]. $\text{Pb}(\text{Mg}_{1/3}\text{Nb}_{2/3})\text{O}_3$ – PbTiO_3 was produced at 1073 K using molten Li_2SO_4 – Na_2SO_4 and NaCl – KCl as a medium of reaction, respectively [28]. $[\text{Pb}(\text{Fe}_{0.5}\text{Nb}_{0.5})\text{O}_3]$ was produced in molten NaCl – KCl at 1073 K for 0.5 h [29]. La-doped NaTaO_3 was produced in molten Na_2SO_4 / K_2SO_4 for 0.5–1 h [30]. Single-crystalline perovskite BaZrO_3 submicrometer-sized particles were obtained using BaC_2O_4 and ZrO_2 as precursors, NaOH/KOH as the molten reaction at 993 K [31]. Rare earth orthoferrites of the general formula LnFeO_3 ($\text{Ln} = \text{La}, \text{Pr}$ and Nd) phases were synthesized in molten NaOH flux at 673 K [32]. As far as we know, however, there are quite a few reports on the synthesis of LaMO_3 perovskites using molten nitrates [33,34]. In this paper, we systematically investigate the effect of salt medium, annealing temperatures (mainly 450–850 °C) and basicity of the melt (NaNO_2 , NaNO_3 – KNO_3 and NaNO_3 – KNO_3 with Na_2O_2) on morphology, composition, size and shape of the product in the synthesis of crystalline LaMO_3 ($M = \text{Fe}, \text{Co}, \text{Ni}$) perovskite particles.

2. Experimental

2.1. Materials and synthesis

Materials: $\text{La}(\text{NO}_3)_3 \cdot 6\text{H}_2\text{O}$ (Tianjin Fu-chen Chemical Reagent Factory, 99%), $\text{Fe}(\text{NO}_3)_3 \cdot 9\text{H}_2\text{O}$ (Shantou Guanghua Chemical Factory, 98.5%), $\text{Co}(\text{NO}_3)_2 \cdot 6\text{H}_2\text{O}$

* Corresponding author. Tel.: +86 020 85220223; fax: +86 020 85220223.

E-mail address: tyangj@jnu.edu.cn (J. Yang).

Table 1
Reaction conditions and results of the synthesis of LaFeO₃ powder in molten salts.

No.	Flux	Temperature (°C)	Products	Color	Crystallite size (nm)	BET area (m ² /g)
01	NaNO ₂	450	LaFeO ₃	Yellowish-brown	21.9	26.54
02	NaNO ₂	550	LaFeO ₃	Yellowish-brown	25.8	21.31
03	NaNO ₂	650	LaFeO ₃	Yellowish-brown	32.3	16.23
04	NaNO ₂	750	LaFeO ₃	Yellowish-brown	51.0	8.27
05	NaNO ₂	850	LaFeO ₃ , La ₂ O ₃	Gray-black	–	–
06	NaNO ₃ –KNO ₃	450	La ₂ O ₃ , Fe ₂ O ₃	Red-brown	–	–
07	NaNO ₃ –KNO ₃	550	LaFeO ₃ , La ₂ O ₃	Red-brown	–	–
08	NaNO ₃ –KNO ₃	650	LaFeO ₃	Yellowish-brown	32.25	12.46
09	NaNO ₃ –KNO ₃	750	LaFeO ₃	Yellowish-brown	47.25	7.23
10	NaNO ₃ –KNO ₃	800	LaFeO ₃	Yellowish-brown	51.15	4.12
11	NaNO ₃ –KNO ₃	850	LaFeO ₃ , La ₂ O ₃ , Fe ₂ O ₃	Yellowish-brown	26.0	8.45
12	NaNO ₃ –KNO ₃ –Na ₂ O ₂	450	LaFeO ₃ , La ₂ O ₃	Black	–	–
13	NaNO ₃ –KNO ₃ –Na ₂ O ₂	550	LaFeO ₃ , La ₂ O ₃	Black	–	–
14	NaNO ₃ –KNO ₃ –Na ₂ O ₂	650	LaFeO ₃ , La ₂ O ₃	Black	–	–
15	NaNO ₃ –KNO ₃ –Na ₂ O ₂	750	LaFeO ₃	Black	36.0	1.76
16	NaNO ₃ –KNO ₃ –Na ₂ O ₂	800	LaFeO ₃	Black	38.4	1.48
17	NaNO ₃ –KNO ₃ –Na ₂ O ₂	850	LaFeO ₃	Gray-black	35.8	–
18	None	450	La ₂ O ₃ , Fe ₂ O ₃	Red-brown	–	–
19	None	800	LaFeO ₃ , La ₂ O ₃	Yellowish-brown	–	7.38

(Tianjin Fu-chen Chemical Reagent Factory, 99%), Ni(NO₃)₂·6H₂O (Tianjin Damao Chemical Reagent Factory, 98.5%), KNO₃ (Guangzhou Chemical Reagent Factory, 99%), NaNO₃ (Tianjin Damao Chemical Reagent Factory, 99%), NaNO₂ (Guangzhou Chemical Reagent Factory, 99%), Na₂O₂ (Tianjin Dagu Chemical Co. Ltd., 92.5%).

La(NO₃)₃·6H₂O was mixed with Fe(NO₃)₃·9H₂O, (Co(NO₃)₂·6H₂O and Ni(NO₃)₂·6H₂O), respectively, with a molar ratio of 1:1. Then NaNO₂, NaNO₃–KNO₃ eutectic (molar ratio 1:1) or NaNO₃–KNO₃ eutectic with Na₂O₂ (molar ratio 2:2:1) as molten salt was mixed with reactants in a molar ratio of La³⁺:M³⁺:NaNO₂ = 1:1:20, La³⁺:M³⁺:NaNO₃–KNO₃ eutectic = 1:1:20 and La³⁺:M³⁺:NaNO₃–KNO₃ eutectic with Na₂O₂ = 1:1:25, respectively. The mixture was placed into the ceramic crucible with a layer of corrosion resistant borosilicate ceramic glaze inside and kept at different temperatures for 2 h in a muffle furnace. After cooling down to room temperature naturally, the soluble compounds of the reaction mixture dissolved in distilled water. The resulting solid product was filtered, washed with distilled water and dried at 120 °C.

2.2. Characterization

The thermal behavior of the powder mixtures was determined by thermogravimetric analysis (TG/DSC) using a SDT Q600 V8.3 Build 101 instrument in an air stream from room temperature to 1000 °C with a heating rate of 10 °C/min. Powder XRD patterns of the LaMO₃ samples were recorded on a Siemens D-5000 diffractometer with monochromatized Cu Kα1 radiation (λ = 0.15405 nm) at 40 kV, 30 mA. SEM images were taken on a JEOL JSM-6330 F scanning electron microscopy. The specific surface area of LaMO₃ was measured through low-temperature N₂ adsorption method (TriStar 3000).

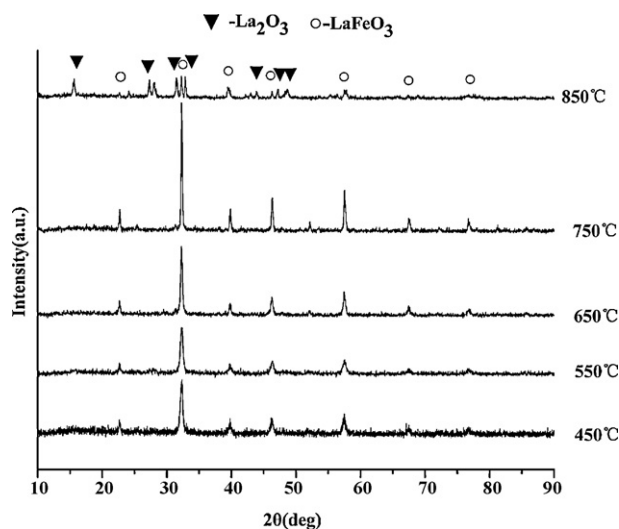


Fig. 1. XRD patterns of samples prepared from La(NO₃)₃·6H₂O–Fe(NO₃)₃·9H₂O in NaNO₂ (system A1).

3. Results and discussion

3.1. Synthesis and characterization of LaFeO₃ nanocrystals

Previously, LaFeO₃ was successfully obtained in molten NaOH at 450 °C for 2 h [32], molten NaNO₂ at 450 °C for 2 h [33] and molten carbonates at 650 °C for 16 h or 550 °C for 12 h in CO₂ atmosphere [34], respectively, using La(NO₃)₃·6H₂O and Fe(NO₃)₃·9H₂O as reactants.

In order to obtain lanthanum ferrite with La:Fe molar ratio 1:1, four systems were tested: La(NO₃)₃·6H₂O–Fe(NO₃)₃·9H₂O in NaNO₂ (A1); NaNO₃–KNO₃ eutectic (B1); NaNO₃–KNO₃ eutectic with Na₂O₂ (C1); La(NO₃)₃·6H₂O–Fe(NO₃)₃·9H₂O without molten salt (D1). The results of the synthesis of LaFeO₃ in molten salts are summarized in Table 1.

In the case of system A1, pure yellowish-brown LaFeO₃ nanocrystals were obtained in the temperature range of 450–750 °C. As shown in Fig. 1, the XRD patterns of samples could be assigned as orthorhombic LaFeO₃ (PDF# 74-2203). No extra peaks were observed in the powder diffraction patterns, indicating that the obtained samples were single phase in nature. The intensity of orthorhombic LaFeO₃ peaks increased with an increase in temperature and the crystallite size increased from 21.9 nm at 450 °C to 51.0 nm at 750 °C, whereas the BET surface area decreased from 26.54 to 8.27 m²/g. If the temperature of the system is higher than the molten salt decomposition, the basicity of the system is no longer controlled. Above 850 °C, gradual trans-

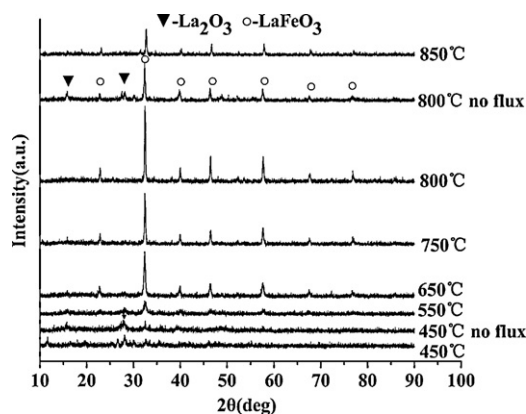


Fig. 2. XRD patterns of samples prepared from La(NO₃)₃·6H₂O–Fe(NO₃)₃·9H₂O in NaNO₃–KNO₃ eutectic (system B1).

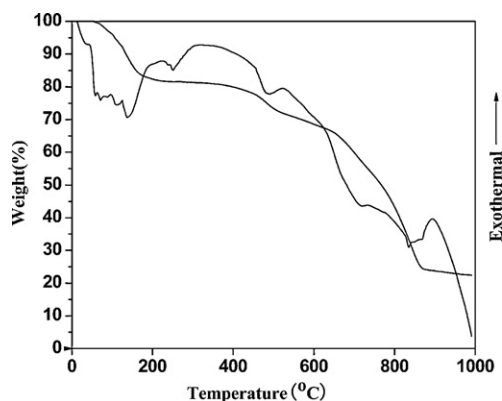


Fig. 3. TG and DSC curves of $\text{La}(\text{NO}_3)_3 \cdot 6\text{H}_2\text{O} - \text{Fe}(\text{NO}_3)_3 \cdot 9\text{H}_2\text{O}$ in $\text{NaNO}_3 - \text{KNO}_3$ eutectic.

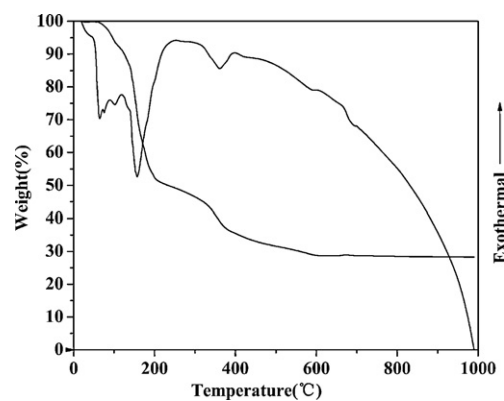


Fig. 4. TG and DSC curves of $\text{La}(\text{NO}_3)_3 \cdot 6\text{H}_2\text{O} - \text{Fe}(\text{NO}_3)_3 \cdot 9\text{H}_2\text{O}$ mixture.

formation of LaFeO_3 to La_2O_3 occurred and a gray-black mixture of LaFeO_3 (black) and La_2O_3 (white) was obtained.

As shown in Fig. 2, in the case of system B1, pure yellowish-brown LaFeO_3 nanocrystals were obtained in the temperature range of 650–800 °C. The TG and DSC curves of the mixture of $\text{La}(\text{NO}_3)_3 \cdot 6\text{H}_2\text{O}$ and $\text{Fe}(\text{NO}_3)_3 \cdot 9\text{H}_2\text{O}$ with and without $\text{NaNO}_3 - \text{KNO}_3$ eutectic are shown in Figs. 3 and 4, respectively. Below 250 °C, removal of the water of crystallization and decomposition of the nitrites cause the weight loss. The weight loss between 300 °C and 450 °C may be regarded as a result of the formation of La_2O_3 on the evidence of the corresponding peaks in the XRD patterns (Fig. 2). Above 450 °C, there is a low change in mass loss (Fig. 4). At 450 °C, the reaction between La_2O_3 and Fe_2O_3 occurred and a very weak signal of LaFeO_3 was recognized in the XRD patterns (Fig. 2). In system B1, LaFeO_3 was almost completely formed at 800 °C, while some signals of La_2O_3 and Fe_2O_3 were still observed in system D1 (without $\text{NaNO}_3 - \text{KNO}_3$ eutectic). This strongly suggests

that the effect of molten $\text{NaNO}_3 - \text{KNO}_3$ eutectic could improve the purity of LaFeO_3 . By raising the temperature to 850 °C, which is over the decomposition temperature of molten salts [33], we could see very weak signals of La_2O_3 and Fe_2O_3 appeared in the XRD patterns.

In order to investigate how the different temperatures affect the microstructure of LaFeO_3 , SEM analyses of samples obtained at 650 °C, 800 °C and 850 °C in $\text{NaNO}_3 - \text{KNO}_3$ eutectic (system B1) and 800 °C without molten salts (system D1) are presented in Fig. 5. It is clear that the samples synthesized at different temperatures and molten salts exhibit varied microstructures in terms of particle size and morphology. SEM pictures show orthorhombic LaFeO_3 is obtained at 800 °C in $\text{NaNO}_3 - \text{KNO}_3$ eutectic and its SEM micrograph (micrograph b) shows agglomerates of cubic nanocrystals.

In system C1, by adding Na_2O_2 , the basicity of $\text{NaNO}_3 - \text{KNO}_3$ eutectic increased [33]. Black LaFeO_3 powders were obtained in the temperature of 450–850 °C. XRD signals (Fig. 6) show that at temperature lower than 750 °C, LaFeO_3 powders were obtained as

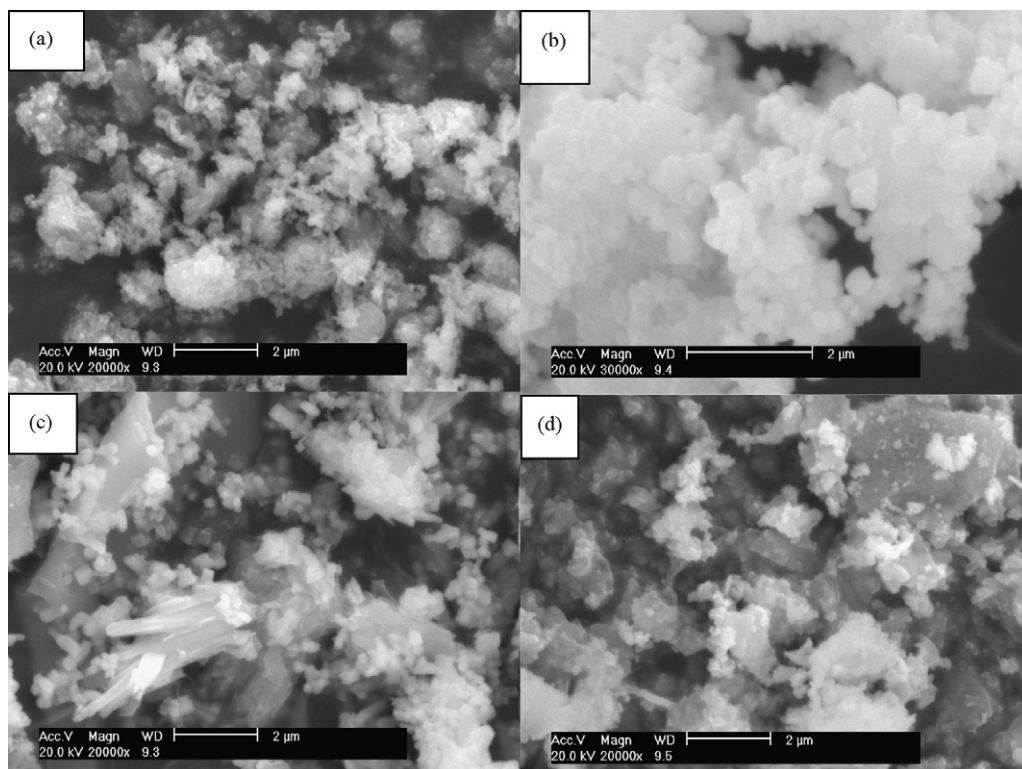


Fig. 5. SEM photographs of LaFeO_3 prepared at (a) 650 °C in $\text{NaNO}_3 - \text{KNO}_3$ eutectic; (b) 800 °C in $\text{NaNO}_3 - \text{KNO}_3$ eutectic; (c) 850 °C in $\text{NaNO}_3 - \text{KNO}_3$ eutectic; (d) 800 °C without $\text{NaNO}_3 - \text{KNO}_3$ eutectic.

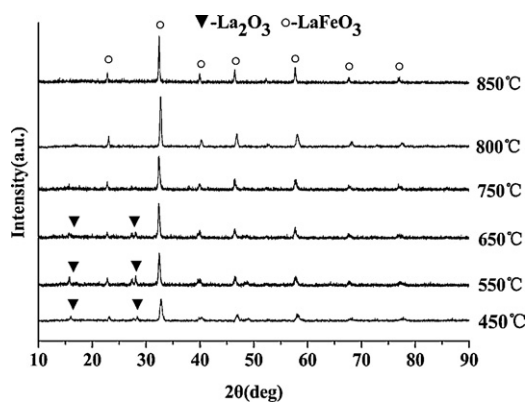


Fig. 6. XRD patterns of samples prepared from $\text{La}(\text{NO}_3)_3 \cdot 6\text{H}_2\text{O} - \text{Fe}(\text{NO}_3)_3 \cdot 9\text{H}_2\text{O}$ in $\text{NaNO}_3 - \text{KNO}_3$ eutectic with Na_2O_2 (system C1).

impure. Compare with system B1, the addition of Na_2O_2 increased the basicity and the ability to stabilise high oxidation states, resulting in the formation of LaFeO_3 at much lower temperature (450–550 °C). However, by further increasing the temperatures over 650 °C, the effect of Na_2O_2 adding on the formation of LaFeO_3 became insignificant. Some researchers reported that lanthanum oxide was a strong base and could be obtained either in molten alkali metal nitrates by adding Na_2O_2 or by raising the temperature over the decomposition temperature [33,35].

3.2. Synthesis and characterization of LaCoO_3 nanocrystals

Previously, LaCoO_3 was obtained as impure powders in molten NaNO_2 at 500 °C for 2 h [33] and molten carbonates at 650 °C for 12 h in $\text{O}_2 : \text{CO}_2 = 1:2$ atmosphere [34], respectively.

Four systems were tested for the synthesis of LaCoO_3 : $\text{La}(\text{NO}_3)_3 \cdot 6\text{H}_2\text{O} - \text{Co}(\text{NO}_3)_2 \cdot 6\text{H}_2\text{O}$ in NaNO_2 (A2), $\text{NaNO}_3 - \text{KNO}_3$ eutectic (B2), $\text{NaNO}_3 - \text{KNO}_3$ eutectic with Na_2O_2 (C2) or $\text{La}(\text{NO}_3)_3 \cdot 6\text{H}_2\text{O} - \text{Co}(\text{NO}_3)_2 \cdot 6\text{H}_2\text{O}$ without molten salt (D2). The results of the LaCoO_3 synthesis in molten salts are summarized in Table 2. We were able to obtain the desired LaCoO_3 compounds.

In system A2, black LaCoO_3 powders were obtained in the temperature of 550–750 °C. As shown in Fig. 7, the XRD of LaCoO_3 could be assigned as hexagonal LaCoO_3 (PDF# 48-0123). The intensity of LaCoO_3 peaks increased with an increase in temperature and the crystallite size increased from 19.3 nm at 550 °C to 28.2 nm at 650 °C, whereas BET surface area decreased from 8.13 to 3.33 m^2/g .

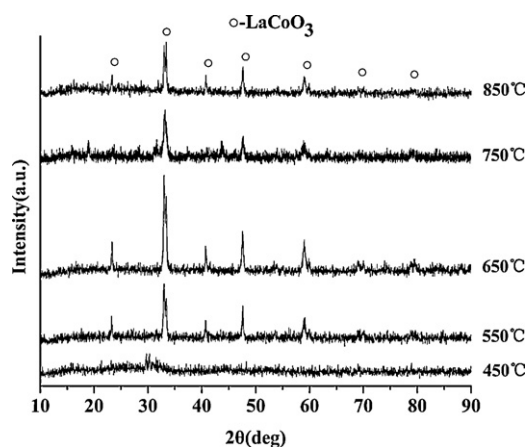


Fig. 7. XRD patterns of samples prepared from $\text{La}(\text{NO}_3)_3 \cdot 6\text{H}_2\text{O} - \text{Co}(\text{NO}_3)_2 \cdot 6\text{H}_2\text{O}$ in NaNO_2 (system A2).

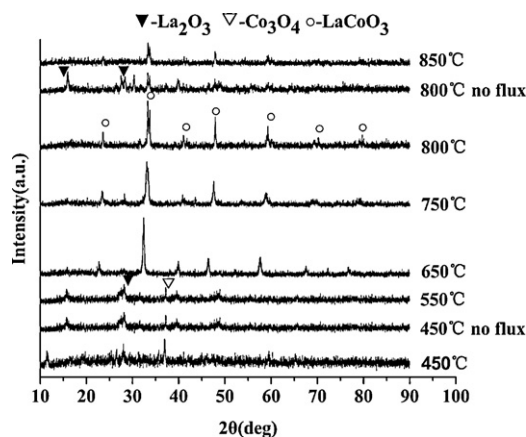


Fig. 8. XRD patterns of samples prepared from $\text{La}(\text{NO}_3)_3 \cdot 6\text{H}_2\text{O} - \text{Co}(\text{NO}_3)_2 \cdot 6\text{H}_2\text{O}$ in $\text{NaNO}_3 - \text{KNO}_3$ eutectic (system B2).

Further increase in temperature to 750 °C, the intensity of LaCoO_3 peaks decreased and crystallite size declined to 20.6 nm.

In system B2, the XRD patterns are shown in Fig. 8. It is obvious that black LaCoO_3 powders were obtained in the temperature of 650–850 °C. When the temperature increased, the color of the samples gradually changed from gray to black. Below 550 °C, a gray mixture of Co_3O_4 and white La_2O_3 was obtained. At 650 °C, the reac-

Table 2
Reaction conditions and results of the synthesis of LaCoO_3 powder in molten salts.

No.	Flux	Temperature (°C)	Products	Color	Crystallite size (nm)	BET area (m^2/g)
01	NaNO_2	450	La_2O_3	Black	–	–
02	NaNO_2	550	LaCoO_3	Black	19.3	8.13
03	NaNO_2	650	LaCoO_3	Black	28.2	3.33
04	NaNO_2	750	LaCoO_3	Black	20.6	–
05	NaNO_2	850	LaCoO_3	Gray	19.2	–
06	$\text{NaNO}_3 - \text{KNO}_3$	450	$\text{Co}_3\text{O}_4, \text{La}_2\text{O}_3$	Gray	–	–
07	$\text{NaNO}_3 - \text{KNO}_3$	550	$\text{Co}_3\text{O}_4, \text{La}_2\text{O}_3$	Dark gray	–	–
08	$\text{NaNO}_3 - \text{KNO}_3$	650	LaCoO_3	Gray-black	23.7	2.43
09	$\text{NaNO}_3 - \text{KNO}_3$	750	LaCoO_3	Black	29.2	1.94
10	$\text{NaNO}_3 - \text{KNO}_3$	800	LaCoO_3	Black	32.5	1.15
11	$\text{NaNO}_3 - \text{KNO}_3$	850	LaCoO_3	Black	–	–
12	$\text{NaNO}_3 - \text{KNO}_3 - \text{Na}_2\text{O}_2$	450	$\text{La}_2\text{O}_3, \text{LaCoO}_3$	Black	–	–
13	$\text{NaNO}_3 - \text{KNO}_3 - \text{Na}_2\text{O}_2$	550	LaCoO_3	Black	49.5	0.67
14	$\text{NaNO}_3 - \text{KNO}_3 - \text{Na}_2\text{O}_2$	650	LaCoO_3	Black	42.9	0.45
15	$\text{NaNO}_3 - \text{KNO}_3 - \text{Na}_2\text{O}_2$	750	LaCoO_3	Black	37.5	0.28
16	$\text{NaNO}_3 - \text{KNO}_3 - \text{Na}_2\text{O}_2$	850	LaCoO_3	Black	–	–
17	None	450	$\text{Co}_3\text{O}_4, \text{La}_2\text{O}_3$	Gray	–	–
18	None	800	$\text{LaCoO}_3, \text{La}_2\text{O}_3$	Black	–	–

tion between La_2O_3 and Co_3O_4 occurred and XRD signals of LaCoO_3 were recognized in the XRD patterns of the samples. In the case of system B2 (with NaNO_3 – KNO_3 eutectic), LaCoO_3 was almost completely formed at 800°C . In contrast to this, La_2O_3 was the main phase observed in system D2 (without eutectic), illustrating the effect of molten NaNO_3 – KNO_3 eutectic could improve the purity of LaCoO_3 . By raising the temperature to 850°C , the intensity of LaCoO_3 peaks decreased, indicating a loss of crystallinity.

In system C2, black LaCoO_3 powders were obtained in the temperature of 550 – 750°C . XRD signals (Fig. 9) show that a single hexagonal phase of LaCoO_3 (PDF# 48-0123) was obtained at 750°C . Compare with system B2, the addition of Na_2O_2 facilitated the reaction between Co_3O_4 and La_2O_3 , leading to the formation of LaCoO_3 at much lower temperature (450 – 550°C). By increasing the temperature, the crystallinity of LaCoO_3 slightly improved and crystallite size increased from 42.5 nm at 550°C to 47.4 nm at 750°C while BET surface area decreased from 0.67 to 0.28 m^2/g . When the temperature rose up to 850°C , the intensity of LaCoO_3 significantly decreased, demonstrating a loss of crystallinity.

SEM micrographs of LaCoO_3 synthesized with different molten salts at different temperatures are presented in Fig. 10. SEM pic-

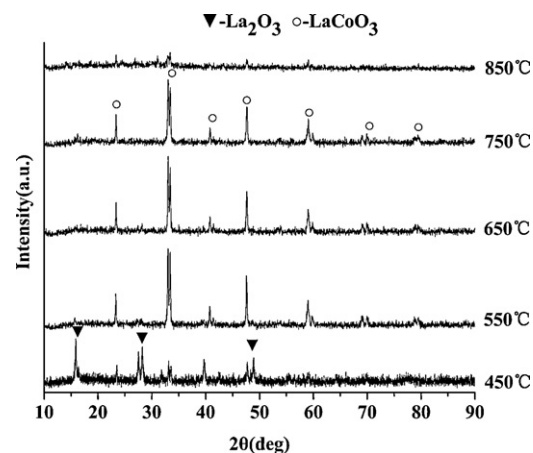


Fig. 9. XRD patterns of samples prepared from $\text{La}(\text{NO}_3)_3 \cdot 6\text{H}_2\text{O}$ – $\text{Co}(\text{NO}_3)_2 \cdot 6\text{H}_2\text{O}$ in NaNO_3 – KNO_3 eutectic with Na_2O_2 (system C2).

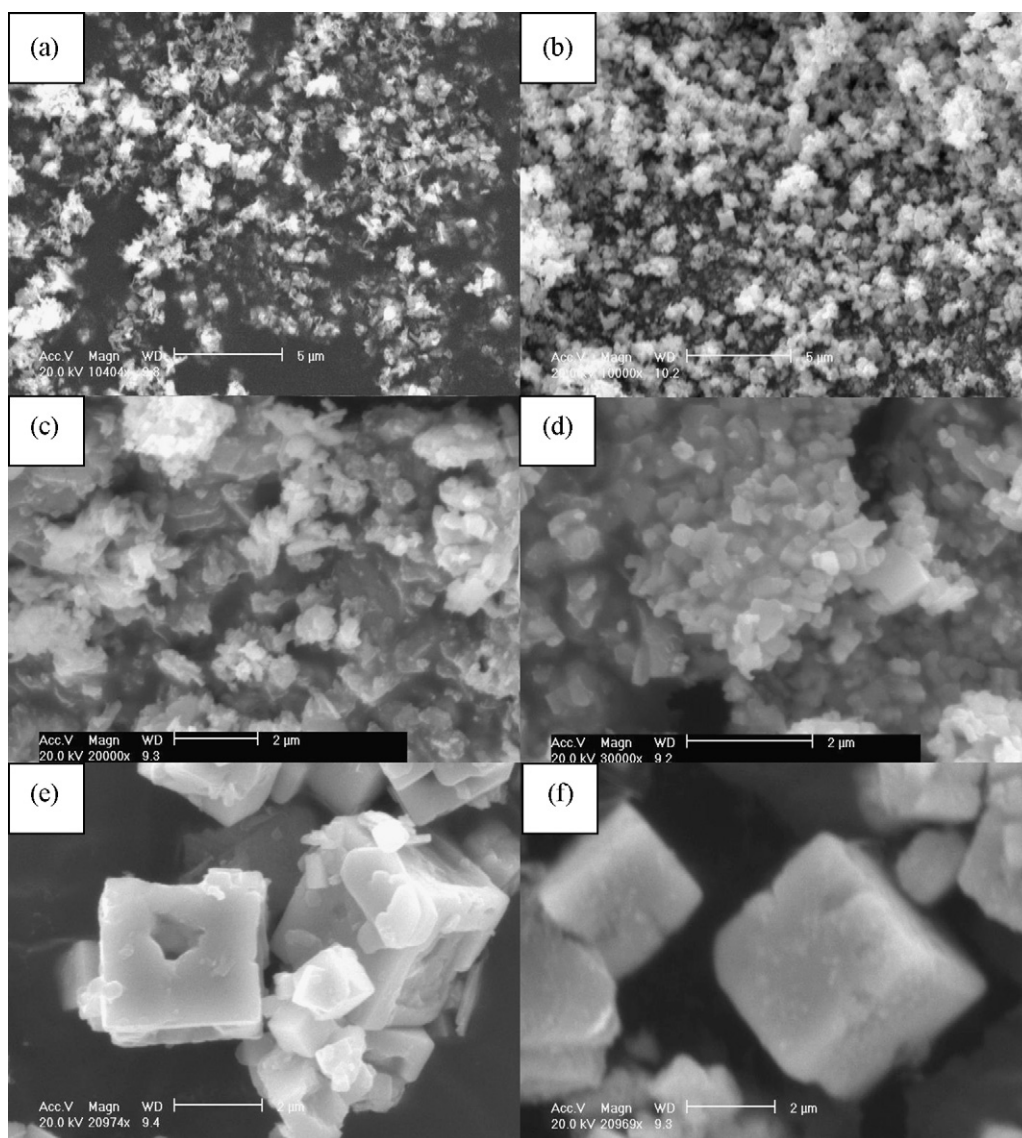


Fig. 10. SEM photographs of LaCoO_3 prepared at (a) 550°C in NaNO_2 flux; (b) 650°C in NaNO_2 flux; (c) 650°C in NaNO_3 – KNO_3 eutectic; (d) 750°C in NaNO_3 – KNO_3 eutectic; (e) 550°C in NaNO_3 – KNO_3 eutectic with Na_2O_2 ; (f) 750°C in NaNO_3 – KNO_3 eutectic with Na_2O_2 .

Table 3
Reaction conditions and results of the synthesis of LaNiO₃ powder in molten salts.

No.	Flux	Temperature (°C)	Products	Color	Crystallite size (nm)	BET area (m ² /g)
01	NaNO ₂	450	La ₂ O ₃ , NiO	Gray-black	–	–
02	NaNO ₂	550	LaNiO ₃ , La ₂ NiO ₄	Black	–	9.39
03	NaNO ₂	650	La ₂ O ₃ , LaNiO ₃	Black	–	–
04	NaNO ₂	750	LaNiO ₃	Black	17.4	4.28
05	NaNO ₂	850	LaNiO ₃ , La ₂ NiO ₄	Black	–	–
06	NaNO ₃ –KNO ₃	450	NiO	Black	–	–
07	NaNO ₃ –KNO ₃	550	La ₂ O ₃ , NiO	Gray	–	–
08	NaNO ₃ –KNO ₃	650	La ₂ O ₃ , NiO	Gray	–	–
09	NaNO ₃ –KNO ₃	750	LaNiO ₃ , La ₂ O ₃	Black	–	–
10	NaNO ₃ –KNO ₃	800	LaNiO ₃ , La ₂ NiO ₄	Black	–	–
11	NaNO ₃ –KNO ₃	850	LaNiO ₃ , La ₂ NiO ₄ , NiO, NiO ₂ , Ni ₂ O ₃	Black	–	–
12	NaNO ₃ –KNO ₃ –Na ₂ O ₂	450	LaNiO ₃ , NiO	Black	–	–
13	NaNO ₃ –KNO ₃ –Na ₂ O ₂	550	LaNiO ₃	Black	36.8	0.05
14	NaNO ₃ –KNO ₃ –Na ₂ O ₂	650	LaNiO ₃	Black	38.6	0.04
15	NaNO ₃ –KNO ₃ –Na ₂ O ₂	750	LaNiO ₃	Black	38.6	0.02
16	NaNO ₃ –KNO ₃ –Na ₂ O ₂	850	LaNiO ₃ , La ₂ O ₃ , NiO, Ni ₂ O ₃	Gray	–	–
17	None	450	La ₂ O ₃ , NiO	Black	–	–
18	None	800	La ₂ O ₃ , LaNiO ₃	Black	–	–

tures show the hexagonal phase of LaCoO₃ samples with cubic morphology was obtained at 550–750 °C in molten NaNO₃–KNO₃ eutectic with Na₂O₂ (Fig. 10e and f). It can be clearly seen that the addition of Na₂O₂ affects the phase transformation and morphology of LaCoO₃. Obviously, the morphology of LaCoO₃ change from agglomerates of spherical particles (system B2) to cubic particles (system C2) and the particle size increases sharply from about 0.63 μm in system B2 at 750 °C to 4.0 μm in system C2 at 750 °C.

3.3. Synthesis and characterization of LaNiO₃ nanocrystals

Like the synthesis of LaFeO₃ and LaCoO₃ powders, four systems were tested: La(NO₃)₃·6H₂O–Ni(NO₃)₂·6H₂O in NaNO₂ (A3), NaNO₃–KNO₃ eutectic (B3), NaNO₃–KNO₃ eutectic with Na₂O₂ (C3) and La(NO₃)₃·6H₂O–Ni(NO₃)₂·6H₂O without molten salt (D3). The results of the LaNiO₃ synthesis in molten salts are summarized in Table 3.

In system A3, LaNiO₃ phase was obtained at a temperature over 550 °C. The XRD pattern of LaNiO₃ (Fig. 11) could be assigned as hexagonal LaNiO₃ (PDF# 33–0711). However, at lower temperature, the hexagonal LaNiO₃ phase did not form completely. It is seen that at 450 °C, only La₂O₃ and NiO phases were recognized in XRD. In the temperature range of 450–650 °C, gradual transformation of La₂O₃ and NiO to hexagonal LaNiO₃ phase occurred and a mixture of LaNiO₃ and La₂O₃ was recognized. Pure hexagonal LaNiO₃ could

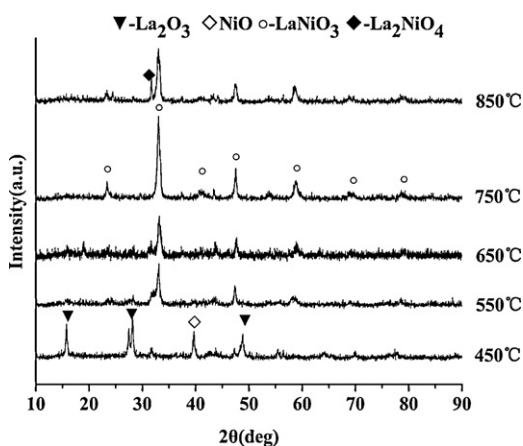


Fig. 11. XRD patterns of samples prepared from La(NO₃)₃·6H₂O–Ni(NO₃)₂·6H₂O in NaNO₂ (system A3).

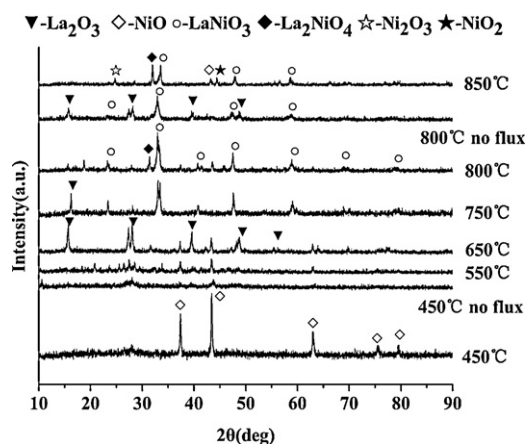


Fig. 12. XRD patterns of samples prepared from La(NO₃)₃·6H₂O–Ni(NO₃)₂·6H₂O in NaNO₃–KNO₃ eutectic (system B3).

only be obtained at 750 °C. Above 850 °C, the intensity of LaNiO₃ significantly decreased and the phase transformation of LaNiO₃ to La₂NiO₄ was observed.

Fig. 12 shows the XRD patterns of the samples prepared in molten NaNO₃–KNO₃ (system B3) at different temperature. At 450 °C, NiO phase was the main phase found in samples and very weak signal of La₂O₃ were observed. In the temperature

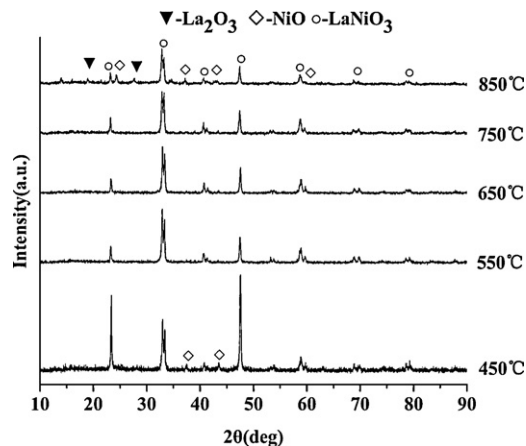


Fig. 13. XRD patterns of samples prepared from La(NO₃)₃·6H₂O–Ni(NO₃)₂·6H₂O in NaNO₃–KNO₃ eutectic with Na₂O₂ (system C3).

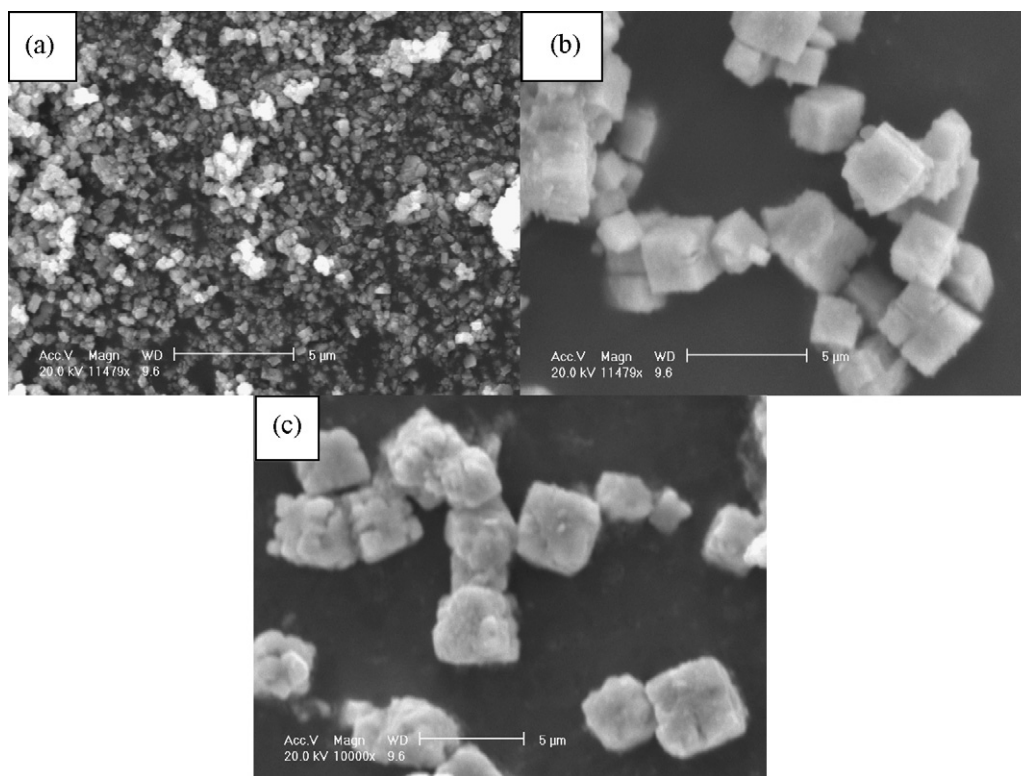


Fig. 14. SEM photographs of LaNiO_3 prepared at (a) 750 °C in NaNO_2 flux; (b) 550 °C in NaNO_3 – KNO_3 eutectic with Na_2O_2 ; (c) 750 °C in NaNO_3 – KNO_3 eutectic with Na_2O_2 .

of 550–650 °C, the intensity of NiO obviously decreased with an increase in temperature, whereas the intensity of La_2O_3 increased. At 750 °C, the reaction between NiO and La_2O_3 occurred and LaNiO_3 was obtained as impure powders. Above 800 °C, transformation of LaNiO_3 phase to La_2NiO_4 phase occurred. At 850 °C, a mixture of LaNiO_3 , La_2NiO_4 , NiO , NiO_2 , and Ni_2O_3 was obtained, indicating the decomposition of LaNiO_3 . In comparison, the phase transformation of La_2O_3 to LaNiO_3 in system D3 (no flux) was much difficult, and strong signals of La_2O_3 are still observed in the XRD patterns in the sample prepared at 800 °C.

Fig. 13 shows the XRD patterns of the samples synthesized in system C3, black LaNiO_3 powders were obtained in the temperature of 450–750 °C. Compare with system B3, the addition of Na_2O_2 facilitated the reaction between La_2O_3 and NiO , leading to the formation of LaNiO_3 at a much lower temperature of 450 °C. Pure hexagonal LaNiO_3 nanocrystals were obtained at 550–750 °C. No extra peaks were observed in the powder diffraction patterns, indicating that the obtained samples were single phase in nature. There is no significant change in the XRD intensity and crystallite size of LaNiO_3 with an increase in temperature from 550 °C to 750 °C. Above 850 °C, the intensity of LaNiO_3 significantly decreased and a mixture of LaNiO_3 , NiO and La_2O_3 was obtained.

Fig. 14 shows the SEM micrographs of LaNiO_3 synthesized in molten NaNO_2 at 750 °C and molten NaNO_3 – KNO_3 eutectic with Na_2O_2 (system C3) at 550 °C and 750 °C. It can be seen that the LaNiO_3 prepared in system C3 has a much larger particle size than that synthesized in molten NaNO_2 . The particle size increases sharply from about 0.20 μm in system A3 at 750 °C to 4.0 μm in system C3 at 750 °C. In the case of system C3, there is no significant change in the morphology or crystallite size of LaNiO_3 in the process of temperature increasing from 550 °C to 750 °C, which is in good agreement with the results of XRD (Fig. 13).

4. Conclusions

LaFeO_3 nanocrystals were successfully synthesized in molten NaNO_2 at 450–750 °C, molten NaNO_3 – KNO_3 at 650–800 °C and molten NaNO_3 – KNO_3 with Na_2O_2 at 800–850 °C for 2 h, respectively.

LaCoO_3 nanocrystals were successfully synthesized in molten NaNO_2 at 550–750 °C, molten NaNO_3 – KNO_3 at 650–850 °C and molten NaNO_3 – KNO_3 with Na_2O_2 at 550–750 °C for 2 h, respectively.

LaNiO_3 nanocrystals were successfully synthesized in molten NaNO_2 at 750 °C, and molten NaNO_3 – KNO_3 with Na_2O_2 at 550–750 °C for 2 h, respectively.

The oxidising properties and basicity of the melt play an important role in the synthesis of LaMO_3 . The addition of Na_2O_2 increased the basicity and the ability to stabilise high oxidation states. With the addition of Na_2O_2 , the morphology of LaCoO_3 synthesized at 750 °C changed from agglomerates of spherical particles (system B2) to cubic particles (system C2) and the particle size increased sharply from about 0.63 μm to 4.0 μm . The LaNiO_3 prepared in NaNO_3 – KNO_3 eutectic with Na_2O_2 had a much larger particle size than that synthesized in molten NaNO_2 .

Acknowledgements

The authors gratefully thank Professor Yulei Zhu and Yu Tang for the valuable discussion, and acknowledge financial support from the Team Project of Guangdong Province Natural Science Foundation (Grant No. 05200555).

References

- [1] Z. Yang, Y. Huang, B. Dong, H.L. Li, *Mater. Res. Bull.* 41 (2006) 274–281.
- [2] C.S. Cheng, L. Zhang, Y.J. Zhang, S.P. Jiang, *Solid State Ionics* 179 (7–8) (2008) 282–289.
- [3] S. Pathak, J. Kuebler, A. Payzant, N. Orlovskaya, *J. Power Sources* 195 (11) (2010) 3612–3620.
- [4] N. Russo, D. Fino, G. Saracco, V. Specchia, *Catal. Today* 137 (2–4) (2008) 306–311.
- [5] J.A. Ruud, M.J. Bowman, K.V. Sarathy, M. Manoharan, A.Y. Ku, V. Ramaswamy, P.R.L. Malenfant, US Patent 2008134895(A1).
- [6] D. Hammer, J. Wu, C. Leighton, *Phys. Rev. B* 69 (13) (2004), 134407/1–134407/11.
- [7] T. Chen, Z.L. Zhou, Y.D. Wang, *Sens. Actuators B: Chem.* 143 (1) (2009) 124–131.
- [8] D. Wang, X.F. Chu, M.L. Gong, *Nanotechnology* 17 (21) (2006) 5501–5505.
- [9] K. Rida, A. Benabbas, F. Bouremmad, M.A. Peña, A. Martínez-Arias, *Catal. Commun.* 7 (2006) 963–968.
- [10] F. Saito, Q.W. Zhang, J. Kano, *J. Mater. Sci.* 39 (2004) 5051–5055.
- [11] W. Zheng, R. Liu, D. Peng, G. Meng, *Mater. Lett.* 43 (2000) 19–22.
- [12] Z.Q. Tian, H.T. Yu, Z.L. Wang, *Mater. Chem. Phys.* 106 (2007) 126–129.
- [13] X. Qi, J. Zhou, Z. Yue, Z. Gui, L. Li, *Ceram. Int.* 29 (2003) 347–349.
- [14] P.V. Gosavi, R.B. Biniwale, *Mater. Chem. Phys.* 119 (1–2) (2010) 324–329.
- [15] K. Rida, A. Benabbas, F. Bouremmad, M.A. Peña, E. Sastre, A. Martínez-Arias, *Appl. Catal. A: Gen.* 327 (2007) 173–179.
- [16] H.Q. Zhong, J. Yang, Y.M. Zhang, *Trans. Nonferr. Metal. Soc.* 19 (1) (2009) 160–166.
- [17] J. Yang, H.Q. Zhong, M. Li, L.Z. Zhang, Y.M. Zhang, *React. Kinet. Catal. Lett.* 97 (2) (2009) 269–274.
- [18] M. Kumar, S. Srikanth, B. Ravikumar, T.C. Alex, S.K. Das, *Mater. Chem. Phys.* 113 (2009) 803–815.
- [19] W. Li, M.W. Zhuo, J.L. Shi, *Mater. Lett.* 58 (2004) 365–368.
- [20] J. Chandradass, Y.J. Cha, K.H. Kim, *Met. Mater. Int.* 15 (6) (2009) 1045–1048.
- [21] M. Popa, J. Frantti, M. Kakihana, *Solid State Ionics* 154–155 (2002) 437–445.
- [22] N. Das, D. Bhattacharya, A. Sen, H.S. Maiti, *Ceram. Int.* 35 (2009) 21–24.
- [23] Z.Q. Tian, W.J. Huang, Y.J. Liang, *Ceram. Int.* 35 (2009) 661–664.
- [24] A.E. Giannakas, A.K. Ladavos, P.J. Pomonis, *Appl. Catal. B: Environ.* 49 (2004) 147–158.
- [25] S. Farhadi, Z. Momeni, M. Taherimehr, *J. Alloys Compd.* 471 (2009) L5–L8.
- [26] N.R. Washburn, A.M. Stacy, A.M. Portis, *Appl. Phys. Lett.* 70 (1997) 1622–1624.
- [27] C. Shivakumara, M.S. Hegde, A.S. Prakash, A.M.A. Khadar, G.N. Subbanna, N.P. Lalla, *Solid State Sci.* 5 (2003) 351–357.
- [28] S.X. Zhao, Q. Li, F.B. Song, C.H. Li, D.Z. Shen, *Key Eng. Mater.* 336–338 (1) (2007) 10–13.
- [29] C.C. Chiu, C.C. Li, S.B. Desu, *J. Am. Ceram. Soc.* 74 (1) (1991) 38–41.
- [30] D.G. Porob, P.A. Maggard, *J. Solid State Chem.* 179 (6) (2006) 1727–1732.
- [31] H.J. Zhou, Y.B. Mao, S.S. Wong, *Chem. Mater.* 19 (2007) 5238–5249.
- [32] C. Shivakumara, *Solid State Commun.* 139 (2006) 165–169.
- [33] C. Matei, D. Berger, P. Marote, S. Stoleriu, J.P. Deloume, *Prog. Solid State Chem.* 35 (2007) 203–209.
- [34] T. Kojima, K. Nomura, Y. Miyazaki, K. Tanimoto, *J. Am. Ceram. Soc.* 89 (2006) 3610–3616.
- [35] D.A. Habboush, D.H. Kerridge, S.A. Tariq, *Thermochim. Acta* 65 (1) (1983) 53–60.